Lattice dynamics of $NaAlH_4$ from high-temperature single-crystal Raman scattering and *ab initio* calculations: Evidence of highly stable AlH_4^- anions

E. H. Majzoub and K. F. McCarty
Sandia National Laboratories, P.O. Box 969, Livermore, California 94551, USA

V. Ozoliņš
Department of Materials Science and Engineering, University of California, Los Angeles, California 90095-1595, USA
(Received 26 August 2004; revised manuscript received 21 October 2004; published 31 January 2005)

Polarized Raman scattering on single crystals of $NaAlH_4$ has been used to determine the symmetry properties and frequencies of the Raman-active vibrational modes over the temperature range from 300 to 425 K, i.e., up to the melting point T_{melt}. Significant softening (by up to 6%) is observed in the modes involving rigid translations of Na^+ cations and translations and librations of AlH_4^-. Surprisingly, the data indicate mode softening of less than 1.5% for the Al-H stretching and Al-H bending modes of the AlH_4^- anion. These results show that the AlH_4^- anion remains a stable structural entity even near the melting point. First-principles linear response calculations of phonon mode frequencies are in reasonably good agreement with the Raman results. The phonon mode Grüneisen parameters, calculated using the quasiharmonic approximation, are found to be significantly higher for the translational and librational modes than for the Al-H bending and stretching modes, but cannot account quantitatively for the dramatic softening observed near T_{melt} in the former two types of modes, suggesting an essentially anharmonic mechanism. The effect of zero-point vibrations on the calculated lattice parameters is found to be large (expansion by 1.2 and 1.5 % in the *a* and *c* parameters, respectively), as expected for a compound with many light elements. We discuss the implications of the observed mode softening for the kinetics of hydrogen release and hypothesize that breaking up the AlH_4^- anions is the rate limiting step. The enhanced kinetics of absorption and desorption in Ti-doped $NaAlH_4$ powders is attributed to the effectiveness of Ti in promoting the breakup of the AlH_4^- anions.

DOI: 10.1103/PhysRevB.71.024118 PACS number(s): 78.30.Hv, 63.20−e, 65.40.De, 77.22.−d

I. INTRODUCTION

Dynamics of hydrogen in solids is a long-standing problems in materials science which provides fascinating opportunities to study the behavior at the boundary between the classical and quantum physics. Hydrogen, being the lightest and the most abundant of all elements, exhibits interesting properties that can be both useful (e.g., efficient solid-state storage) and detrimental (e.g., hydrogen embrittlement) in practical applications. From a theoretical perspective, describing the behavior of hydrogen from the first principles has always been a challenge because the simple classical point-particle treatment is often a poor approximation due to the delocalized nature of the protonic wave function. Experimental studies of hydrogen dynamics are invaluable for calibrating the accuracy of the various *ab initio* computational methods that aim to incorporate the nonclassical nature of hydrogen in modern electronic structure studies.

This paper deals with the lattice dynamics of sodium aluminum tetrahydride, $NaAlH_4$, often referred to as sodium alanate. $NaAlH_4$ crystallizes in an ionic structure containing Na^+ cations and AlH_4^- anions, arranged in an ordered manner on the vertices of a tetragonally deformed face-centered cubic lattice. Bonding within the AlH_4^- (Ref. 1) groups is best characterized as polar covalent (a detailed discussion of the electronic structure and crystal bonding can be found in Refs. 2 and 3). Sodium alanate is a representative of a family of complex hydrides of the $A_n(MH_4)^n$ type, where *A* is a metal of valence *n*, and *M* is a trivalent element, such as B, Al, or Ga.[1] These hydrides have been known for decades, but have attracted relatively little attention until the seminal discovery of Bogdanovič *et al.*[4] that, in the presence of transitional metal catalysts, the material can reversibly release and absorb hydrogen at ambient temperatures and pressures. Metal-doped complex hydrides represent a new paradigm for solid-state hydrogen storage, promising a dramatic increase in the reversibly stored hydrogen weight fraction over traditional metal hydrides. The decomposition reaction proceeds in two steps, first into the sodium aluminum hexahydride Na_3AlH_6, which further decomposes into NaH:

$$NaAlH_4 \rightleftharpoons \tfrac{1}{3}Na_3AlH_6 + \tfrac{2}{3}Al + H_2, \quad (1)$$

$$Na_3AlH_6 \rightleftharpoons 3NaH + Al + \tfrac{3}{2}H_2. \quad (2)$$

These reactions result in about 5.5 wt % of available hydrogen, surpassing all other known inexpensive materials. The system has reasonable kinetics only upon doping with a few mol. % of transition metals, with Ti the preferred choice.[5] The Ti-halide doped samples begin to decompose at pragmatic rates at temperatures of about 80–90 °C,[6] well below the melting point of the compound at about 180 °C.[7,8]

The mechanism of enhanced kinetics in Ti-doped samples is not yet understood, remaining one of the most important obstacles towards developing other material/catalyst combinations with improved kinetics and higher hydrogen weight fraction. Numerous authors[2,6,9–16] have performed kinetic and structural measurements on Ti-doped powdered samples,

often reaching contradictory conclusions about the role of Ti. Here, we adopt a different approach and ask instead what happens in a sample that is *not* doped with Ti as one approaches and exceeds the thermodynamic transition temperature for the decomposition reactions (1)? Surprisingly, the dynamical properties of single-crystal $NaAlH_4$ have not yet been investigated. Adopting this approach, we can characterize the dynamical properties and structural stability of the AlH_4^- anion that is intrinsic to the bulk material, and glean valuable insights into what could be the rate-limiting physical processes associated with reactions (1) and (2). The stability of the AlH_4^- anion is of particular interest, as it can help to clarify the role of the transition metal dopant, and can be probed directly using Raman spectroscopy.[17]

We have grown single crystals of sodium alanate and performed *in situ* Raman scattering measurements up to, and slightly beyond, the melting temperature of this compound. Use of high-quality single crystals allows us to accurately identify the symmetries of the phonon modes and investigate the temperature dependence of their frequencies. The Raman results are compared with the predictions of state-of-the-art *ab initio* density functional theory (DFT) linear response calculations of harmonic phonon frequencies and quasiharmonic Grüneisen parameters. We find that the phonon modes separate neatly into four groups, best described as translational, librational, Al-H bending, and Al-H stretching modes, in agreement with previous Raman studies on *powdered* $NaAlH_4$.[19] Of these modes, the former two exhibit dramatic softening in the narrow interval from room temperature to the melting point, indicating the presence of very large anharmonic effects beyond the "normal" softening associated with lattice expansion. In contrast, the high-frequency modes, corresponding to deformations of the AlH_4^{-1} tetrahedra, show a weak temperature dependence, indicating that the thermal excitation energies available at ambient temperatures are too low to compete with the strong chemical bonding within these molecular units. Since the decomposition of $NaAlH_4$ requires breaking up of the AlH_4^{-1} units and rebonding some of them into an octahedral coordination to form Na_3AlH_6, and both of these processes have to happen well below the melting temperature, our results suggest that this breakup is the rate-limiting step in reaction (1).

II. METHODS

A. Experiments

Single crystal samples of $NaAlH_4$ were grown by solvent evaporation from *Sigma Aldrich* 1 M solutions of $NaAlH_4$ in THF. The crystals were grown in capped vials of diameter 20 mm and a height of 50 mm. Typically 10 ml of 1 M solution was used for evaporation.

Multiple nuclei were often observed, and assumed to be due to impurities in the as-received solution, and resulted in the formation of many crystals of dimension 0.1–0.5 mm. The following procedure was employed to produce larger crystals. A vial prepared with solution as above was allowed to evaporate to the saturation point of $NaAlH_4$ in THF, about 3 mols/l.[5] Many crystallites formed in this solution and removed many of the nucleation sites. This supersaturated solution was then gently removed to a clean vial and a previously prepared and selected 0.5–1 mm crystal was placed in the supersaturated solution and used as a seed. Although additional nucleation occurred in the seeded solution, the resulting seed crystal typically grew to around 2 mm in dimension.

Raman data were collected on a Spex model 1877 0.6 m triple spectrometer, using the 514 nm line of a Coherent Innova Ar ion laser, at a power of about 10 mW at the sample. The spectrometer efficiency ratio for horizontal and vertical polarizations was corrected for in the polarized spectra. Spectrometer and filter gratings were 1800 and 600 lines/mm, respectively.

All spectra were collected in 180° backscattering geometry utilizing a microprobe apparatus consisting of a 20× objective to focus the incident light and collect the scattered light. Polarization data are described using Porto notation, such as $z(xy)\bar{z}$, indicating that the incident and scattered light travel along the z and $\bar{z}$ direction, and the incident and scattered polarizations are x and y, respectively. These directions correspond to the laboratory frame with the crystal orientation described below.

The high-temperature *in situ* cell consisted of a cylindrical platinum sample pan of approximately 7 mm in diameter and 5 mm in depth, with one end open to allow for entry and exit of the laser beam. The platinum pan was enclosed in an alumina cup surrounded by a heating coil. A water-cooled stainless steel housing enclosed the sample holder and had a fused silica window on one end. A constant flow of approximately 3-5 cc/sec of ultra-high purity Ar was maintained through the cell during the *in situ* measurement. A type-K thermocouple bead was held in contact with the bottom of the pan, upon which rested the crystal. The temperature measurements were approximate because of nonideal thermal contact between the sample and the thermocouple or sample pan.

B. *Ab initio* calculations

Ab initio calculations of phonon spectra were performed using the density functional theory (DFT) linear response method.[20] We used norm conserving pseudopotentials generated according to the Troullier-Martins prescription,[21] including the Louie-Froyen-Cohen[22] nonlinear core correction for Na and Al. Wave functions were expanded in a plane wave basis set with an energy cutoff $E_{\mathrm{cut}}=680$ eV. A regular $8\times8\times8$ k-point mesh was used for sampling the electronic states in the Brillouin zone of the body-centered tetragonal unit cell of $NaAlH_4$. The structural properties and formation energies calculated with both the local-density approximation (LDA) and the generalized gradient approximation (GGA) have been given in an earlier publication.[2] Born effective charges $Z^*_{\alpha\beta}(i)$ describing the macroscopic polarization induced by ionic displacements in optical phonons, and the high-frequency dielectric tensor $\epsilon^{\infty}_{\alpha\beta}$ were calculated using the linear response formalism.[20] Due to the large band gap of $NaAlH_4$ (about 5 eV), the $8\times8\times8$ k-point mesh was more than sufficient to obtain very accurate dielectric properties. Decreasing the sampling mesh to $6\times6\times6$ produced negligible (approximately 1%) variations in the calculated $\epsilon^{\infty}_{\alpha\beta}$.

Phonon mode Grüneisen parameters $\gamma = \partial \ln \omega / \partial \ln a$, where ω is the phonon frequency, were estimated using the quasiharmonic approximation. We considered changes in both the overall volume at $c/a = \text{const}$ and in the c/a ratio at $V = \text{const}$, where c and a are the lattice parameters for this body-centered tetragonal crystal. For each, we took an increase of approximately 2% and subsequently performed a relaxation of hydrogen positions (metal ion positions are fixed by symmetry). Phonon frequencies were calculated on a $4 \times 4 \times 4$ phonon wave vector grid. Using standard expressions for the vibrational free energy, we expressed the latter as a linear function of lattice parameters a and c, and a nonlinear interpolating function of the temperature. We also parametrized the total static lattice energy as a function of both a and c. For each temperature, the minimum of the total free energy (static lattice + vibrational) yielded the lattice parameters as functions of T. In principle, a fully consistent quasiharmonic treatment also requires the evaluation of the Grüneisen parameters corresponding to changes in hydrogen coordinates. However, such a tedious undertaking is expected to matter only for the high-frequency Al-H bond-stretching and H-Al-H bond-bending modes. Since the thermal population of these modes is low even at the melting temperature of the compound, the effects on the lattice parameters and quasiharmonic mode softening are expected to be small.

For $NaAlH_4$, it has been shown that the generalized gradient approximation (GGA) gives noticeably better structural properties and formation energies than the LDA.[2] It is also reasonable to expect that the GGA will give better phonon frequencies if the calculations are performed at the predicted GGA lattice parameters. Unfortunately, since the GGA is not implemented in our linear response code, we had to resort to frozen phonon calculations using the Vienna *ab initio* Simulation Package (VASP) developed at the Institut für Materialphysik of the Universität Wien.[23–27] We obtained all the $q = 0$ phonon states using the unit cell of $NaAlH_4$ and calculating all seven (two each for Na and Al and three for H) symmetry inequivalent rows of the $\mathbf{q} = 0$ dynamical matrix. Individual elements $D^{ij}_{\alpha\beta}$ of the $\mathbf{q} = 0$ dynamical matrix are proportional to the force acting on the atom i along the Cartesian direction α if the atom j is displaced by a small amount along the direction β, $F^i_\alpha = -\sqrt{M_i M_j} D^{ij}_{\alpha\beta} u^i_\beta$. For each symmetry-inequivalent choice of u^j_β, the forces F^i_α were obtained for a set of 11 evenly distributed displacements around the equilibrium position, from $u^j_\beta = -0.1$ to $+0.1$ with a step of 0.02 Å. The calculated Hellman-Feynman forces were fit using third-order splines, and the linear terms were used to extract $D^{ij}_{\alpha\beta}$. We encountered annoying numerical issues when extracting accurate values of $D^{ij}_{\alpha\beta}$ associated with the movement of Na atoms, caused by small, seemingly random fluctuations in the Hellmann-Feynman forces at the level of 0.02 eV/Å. The origin of these numerical errors is not clear. We estimate that the frequencies of the lowest (translational) phonon modes, listed in Table I, have a numerical uncertainty of approximately 10 cm^{-1}. This uncertainty is small enough so that a meaningful comparison with experimental Raman data is possible. However, we were not able to extract the Grüneisen parameters from GGA frozen phonon calculations for the translational modes as the noise was on the same level as the quasiharmonic softening. In contrast, our linear response LDA results are numerically accurate to a few cm^{-1}, i.e., increasing the plane wave cutoff energy, the number of k points or the degree of convergence would result in very small changes in the calculated frequencies.

The important question of physical accuracy is much more complex, as there are several effects which are either approximated or not included in these kinds of calculations. Among the latter, use of approximate exchange-correlation functionals (LDA or GGA) and quasi-harmonic treatment of anharmonic vibrational effects are the most serious. Note that the calculations are performed at the predicted equilibrium geometry (obtained from LDA or GGA) for a static *nonvibrating* lattice. Effect of atomic vibrations on the lattice parameters is taken into account via phonon mode Grüneisen parameters, which allow us to evaluate both the $T = 0$ K lattice expansion due to zero-point vibrations and the $T > 0$ coefficient of thermal expansion. Our treatment includes the changes in effective interatomic force constants due to lattice expansion, but neglects intrinsically anharmonic effects, such those associated with phonon-phonon interactions and finite phonon lifetimes. The quasiharmonic approximation is expected to become increasingly worse upon approaching the melting temperature, which for $NaAlH_4$ is around $T = 180$ °C. Since the crystal melts by disintegrating into Na^+ cations and AlH_4^- anions, it is expected that near the melting temperature the translational displacements and rotations of the AlH_4^- units become very large, and thus the importance of intrinsic anharmonic effects (i.e., of those beyond the simple quasiharmonic lattice expansion) for the low-energy modes should also increase. The magnitude of these effects could be quantified using *ab initio* molecular dynamics (MD) simulations, which we unfortunately found to be impractically time consuming, and possibly lacking in physical accuracy due to the neglect of the quantum-mechanical nature of hydrogen ions in MD. Further studies based upon a fully quantum-mechanical treatment of the H ions, such as the path integral approach,[28] would help to clarify whether the existing discrepancies between the calculated and measured lattice parameters and phonon frequencies can be attributed to the approximate exchange correlation, to the approximate treatment of the hydrogen dynamics, or both.

III. RESULTS

A. Mode assignments from polarized Raman spectra

The crystal structure of $NaAlH_4$ is body-centered tetragonal with the space group $I4_{1/a}$.[29,30] The prepared $NaAlH_4$ single crystals were square pyramidal in morphology, with the largest facets being (101) planes. This crystal habit is related to that of scheelite, with prototype structure $CaWO_4$. The scattering geometry had the incident and scattered light along the normal to the (101) facet. The vibrational mode structure of this crystal can be determined from the correlation method,[31] with the following result:

$$\Gamma^{\text{tot}}_{\text{vib}} = 3A_g + 5B_g + 5E_g + 3A_u + 3B_u + 3E_u. \qquad (3)$$

$NaAlH_4$ is centrosymmetric, therefore all even ("gerade") modes are Raman active, and all odd modes are infrared

TABLE I. Measured Raman mode frequencies from the (101) face in single crystal $NaAlH_4$ in cm^{-1}. Horizontal lines in the table separate, from lowest to highest wave number, modes attributed to translation, libration, Al-H bending, and Al-H stretching modes, respectively. All data were taken at temperature of approximately 22.5 °C. The fitted peak position errors are shown only when they are greater than or equal to 1 cm^{-1}. The last column lists the phonon mode Grüneisen parameters for a uniform change in volume $\gamma = (\partial \ln \omega / \partial \ln V)$, calculated using the LDA linear response method.

Mode	Polarization				*Ab initio* calculations		
symmetry	*xx*	*xy*	*yx*	*yy*	LDA	GGA	γ_G
			Translational modes				
E_g	117	117	117		135	116	1.4
B_g	125	125	125	125	128	101	0.7
E_g	184	184	184		210	191	1.0
B_g[a]				184	220	182	1.7
			Librational modes				
A_g	432.5			432.5	512	458	0.9
E_g	524	524	525±1		614	560	0.8
			Al-H bending modes				
A_g	771			765±1	759	748	0.5
B_g		817±1	815±2	813±1	786	797	0.3
E_g[a]		848±3	851±4		822	817	0.7
B_g[b]					844	850	0.5
			Al-H stretching modes				
E_g	1684	1687	1687		1681	1649	0.3
A_g	1774			1773	1729	1726	0.2
B_g[a]		1782	1782±3		1706	1673	0.3

[a]Tentative assignment.
[b]Unable to assign.

active, according to the rule of mutual exclusion. The Raman polarizability tensors for the crystal class $4/m$ C_{4h}, for the irreducible representations A_g, B_g, and E_g, respectively, are

$$A_g: \begin{pmatrix} a & 0 & 0 \\ 0 & a & 0 \\ 0 & 0 & b \end{pmatrix}, \quad B_g: \begin{pmatrix} c & d & 0 \\ d & -c & 0 \\ 0 & 0 & 0 \end{pmatrix}, \quad E_g: \begin{pmatrix} 0 & 0 & e \\ 0 & 0 & f \\ e & f & 0 \end{pmatrix}. \tag{4}$$

The tensors, after transformation to a coordinate system with the [101] direction pointing along the laboratory z axis (a rotation of the crystal about the laboratory y axis by $\phi = 1.1537$ rad), become

$$A_g: \begin{pmatrix} 0.8b + 0.2a & 0 & 0.4a - 0.4b \\ 0 & a & 0 \\ 0.4a - 0.4b & 0 & 0.2b + 0.8a \end{pmatrix}, \tag{5}$$

$$B_g: \begin{pmatrix} 0.16c & 0.41d & 0.37c \\ 0.41d & -c & 0.91d \\ 0.37c & 0.91d & 0.84c \end{pmatrix}, \tag{6}$$

$$E_g: \begin{pmatrix} -0.74e & -0.91f & -0.67e \\ -0.91f & 0 & 0.41f \\ -0.67e & 0.41f & 0.74e \end{pmatrix}. \tag{7}$$

While no polarization configuration in this scattering geometry allows a single symmetry to be exclusively allowed, we will show that careful experimental analysis combined with first-principles calculations of phonon frequencies allow us to experimentally identify most of the Raman-active phonons. It can be seen from the transformed polarization tensors in Eqs. (5)–(7) that A_g modes will have no mixed components (xy or yx). A_g modes represent motion of hydrogen atoms only. Both E_g and B_g modes result in hydrogen atom motion, but differ in the motion of the metal atoms. E_g modes will have no yy component, and correspond to Na and Al motion perpendicular to the c axis of the crystal. B_g modes can have all components of polarization for this crystal face, and correspond to Na and Al motions parallel to the c axis.

The class of $4d/5d$ oxides isostructural to $CaWO_4$ has been investigated by Porto *et al.* (Ref. 18, and references therein). The phonon modes of these oxides are well described by "external" modes, where the XO_4^{--} ions are considered rigid structural units, and "internal" modes, in which the the ions undergo molecularlike vibrations about a stationary center of mass. We show that the $NaAlH_4$ crystal can be described in the same manner.

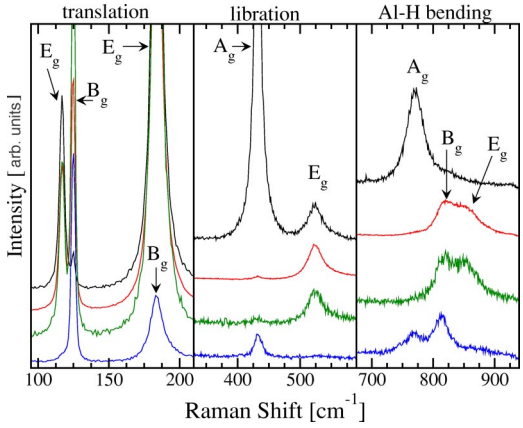

FIG. 1. (Color online) Raman spectra from the (101) face of single crystal $NaAlH_4$, showing the bending and libration modes of the AlH_4^{-1} anion, and the translational modes at the lowest values of the wave number. For clarity, the intensity scales are different in the three panels and the spectra are offset. In each panel, the polarizations are *xx*, *xy*, *yx*, and *yy*, from top to bottom.

The measured Raman spectra at room temperature are given in Figs. 1 and 2. The extracted values for the mode frequencies at room temperature are given in Table I. While the vibrational modes corresponding to Al-H stretching, bending, libration of the AlH_4^{-1} anion, and translational modes were determined previously on powdered samples,[19] a polarization analysis of single crystal samples is required for unambiguous mode symmetry identification and to distinguish overlapping vibrational modes. The data peaks were fit to pseudo-Voigt profiles. The fitting errors shown do not represent the instrumental resolution of the spectrometer, which is approximately 1 cm^{-1}. Some of the peak positions are strongly temperature dependent, as shown in the next section.

Translation modes. The four modes of lowest frequency correspond to translational modes. The mode at approximately 117 cm^{-1} consists of strong contributions from *xx*, *xy*, and *yx*, and essentially no intensity in *yy*, and was therefore assigned to E_g. Because the next mode, located at about 125 cm^{-1}, has a very diminished *xx* component relative to the other polarizations, it is assigned to B_g. The peak at 184 cm^{-1} has strong intensity in the *xx*, *xy*, and *yx* polarizations, consistent with an E_g mode. However, the peak at 184 cm^{-1} also contains some intensity in *yy* polarization, which cannot come from an E_g mode. Analysis shows that the *yy* intensity is greater than expected from "leakage" of the E_g mode due to misalignment of the crystal. The intensity in the *yy* polarization of the E_g mode at 117 cm^{-1} is about 24 times weaker than the *xx* polarization intensity. In contrast, the *yy* intensity of the 184 cm^{-1} peak is about 9 times weaker than the *xx* intensity. The large difference in the *xx* and *yy* intensity ratios for the two peaks suggest that the 184 cm^{-1} peak contains a B_g mode in addition to the clear E_g mode. We note that this assignment is tentative.

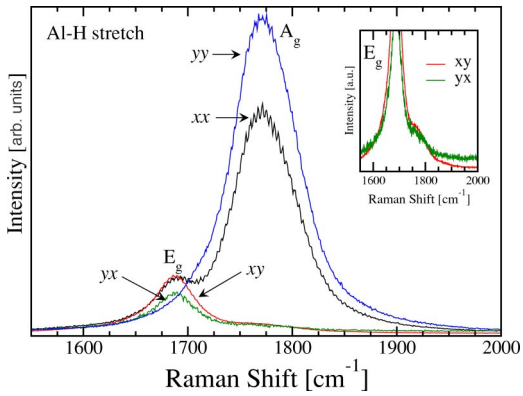

FIG. 2. (Color online) Raman spectra from the (101) face of single crystal $NaAlH_4$, showing the Al-H stretching modes. The inset arrow shows the shoulder on the E_g modes in the *xy* and *yx* polarizations where the B_g mode may be located.

Libration modes. The mode at about 432 cm^{-1} is assigned to A_g. Any intensity in the mixed polarizations is attributed to leakage due to slightly misaligned crystal or polarizer settings. Because there is no intensity in the *yy* polarization, the mode at about 524 cm^{-1} is clearly E_g.

Al-H bending modes. The peak at about 767 cm^{-1} has strong *xx* and *yy* intensity and no intensity in crossed polarization (*xy* and *yx*). Therefore it is an A_g mode. The crossed polarization spectra show a broad band around 825 cm^{-1} with at least two peaks. This band must arise from B_g or E_g modes. The peak at about 815 cm^{-1} shows intensity in *yy* polarization and some intensity in *xx* polarization, establishing it as a B_g mode. Assigning the intensity near 849 cm^{-1} is problematic—it arises from either a B_g mode with small matrix element *c* or an E_g mode with small matrix element *e*, as shown in Eqs. (6) and (7). Furthermore, the calculations show that there is a B_g mode and E_g mode in this vicinity. Because the other B_g modes have strong *yy* intensity, we tentatively assign the 849 cm^{-1} peak, with its weak *yy* intensity, to E_g. We note that the peak may contain intensity from the B_g mode.

Al-H stretching modes. The *yy* component shown in Fig. 2 can be fit well by a pseudo-Voigt line shape. The strong *yy* and *xx* components at about 1773 cm^{-1} are therefore assigned to A_g. The lack of *yy* component at about 1683–1687 cm^{-1} clearly indicates that this mode is E_g. A fit to the peak positions of the remaining intensity under the strong A_g mode, shown in the inset, yields a slightly different Raman shift of about 1781–1782 cm^{-1}, and is assigned to B_g. The B_g assignment here may be incorrect and the intensity in the mixed polarizations the result of mode leakage from slight misorientation of the crystal or polarizers.

B. High-temperature Raman spectra—Structural stability

Nonpolarized spectra were collected for *in situ* measurements as a function of temperature. The crystal of $NaAlH_4$ used in the *in situ* measurement was observed to begin decomposing, with surface melting and bubbling, presumably from hydrogen outgassing, when the thermocouple measured about 161 °C, which we refer to as the "apparent" melting temperature. The melting temperature of $NaAlH_4$ by our own differential scanning calorimetry measurements is 180.5±0.5 °C. We believe the difference is due to the flow of

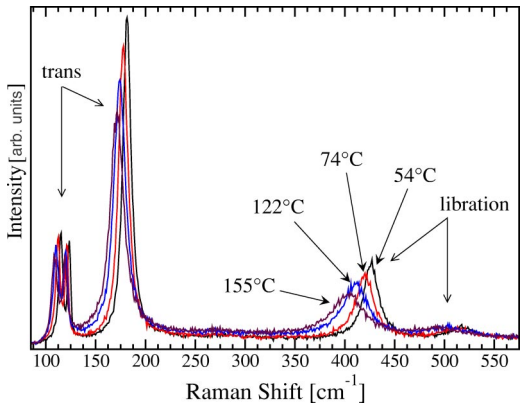

FIG. 3. (Color online) Unpolarized Raman spectra from single crystal $NaAlH_4$ at varying temperature, showing softening of the librational and translational modes, indicated by a shift to lower wave number.

argon in our Raman test cell. Results of the *in situ* measurements are shown in Figs. 3 and 4. Mode softening is evidenced by a shifting of the vibration frequency to lower values of the wave number. This indicates that the force constants between atoms involved in these modes are becoming weaker, as a result of lattice expansion and anharmonic effects.

The data indicate that the Al-H bending and stretching modes are not softening nearly to the extent observed for the libration and translational modes. Figure 5 shows the shifts of fitted peak positions as a function of temperature. In cases where the modes overlapped, such as the A_g and B_g modes at about 1773 cm^{-1}, the peaks observed were fitted to a single pseudo-Voigt profile. The E_g libration modes were difficult to fit and resulted in large error bars; however, their shifting to lower wave number with temperature increase is clearly visible in Fig. 3. Note that the Al-H bending and stretching modes shift less than 2% from their room temperature values up to the melting point of $NaAlH_4$. This suggests that the AlH_4^- anion is a stable structure up to the melting point. In fact, slightly below about 161 °C, the Raman modes associated with the crystal lattice completely disappeared while the AlH_4^- anion modes persisted, as shown in Fig. 6. This observation establishes that AlH_4^- persists as a stable molecular species even after the $NaAlH_4$ lattice is lost.

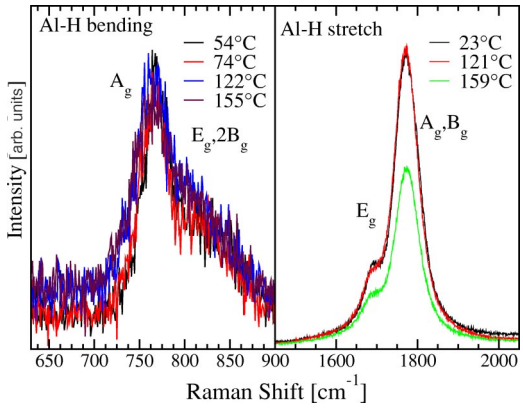

FIG. 4. (Color online) Unpolarized Raman spectra from single crystal $NaAlH_4$ at varying temperature, showing only slight softening of the bending and stretching modes of the AlH_4^{-1} anion.

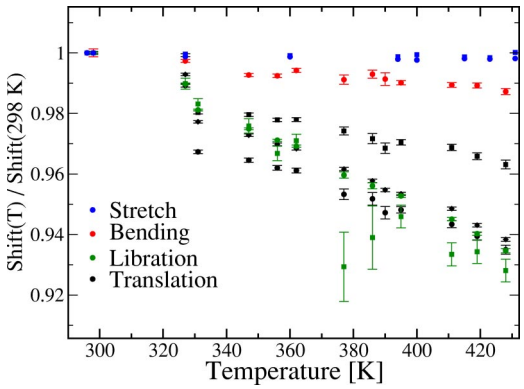

FIG. 5. (Color online) Fitted values for the vibrational modes as a function of temperature. The modes are color coded for each of the groups: translation (black), libration (green), bending (red), and stretching (blue). The bending and stretching modes of the AlH_4^- anion shift less than 2% from their room-temperature values at the melting point of the compound.

C. Results of *ab initio* calculations

The calculated phonon frequencies using the LDA and GGA are given in Table I, and the corresponding eigenvectors are shown in Figs. 7–10 below. Each set of phonon frequencies was calculated at the static equilibrium lattice parameters predicted by the LDA and GGA, respectively. Since the latter are several percent smaller than the experimental values, the calculated LDA frequencies are expected to be somewhat higher than the experimental values, a well-known problem of the LDA which also manifests itself in Table I. Overall, the quantitative agreement between the GGA frequencies and the experimental Raman data is better, but far from perfect. We attribute this to the neglect of thermal expansion and zero-point vibrations in the calculated

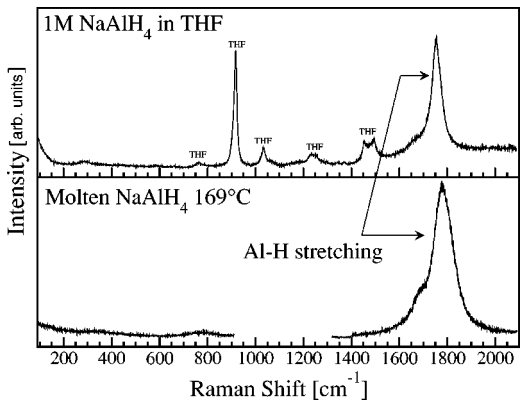

FIG. 6. The bottom panel is Raman spectra of the surface melt of $NaAlH_4$ at 169 °C. The apparent melting temperature of the crystal was 161 °C. The AlH_4^- anion is still clearly intact, indicating that the molecular unit is stable in the melt, where the loss of crystal periodicity destroys the translational and librational modes. The top panel illustrates vibrations of the AlH_4^- anion in a 1 M solution of $NaAlH_4$ in tetrahydrofuran (THF) for reference.

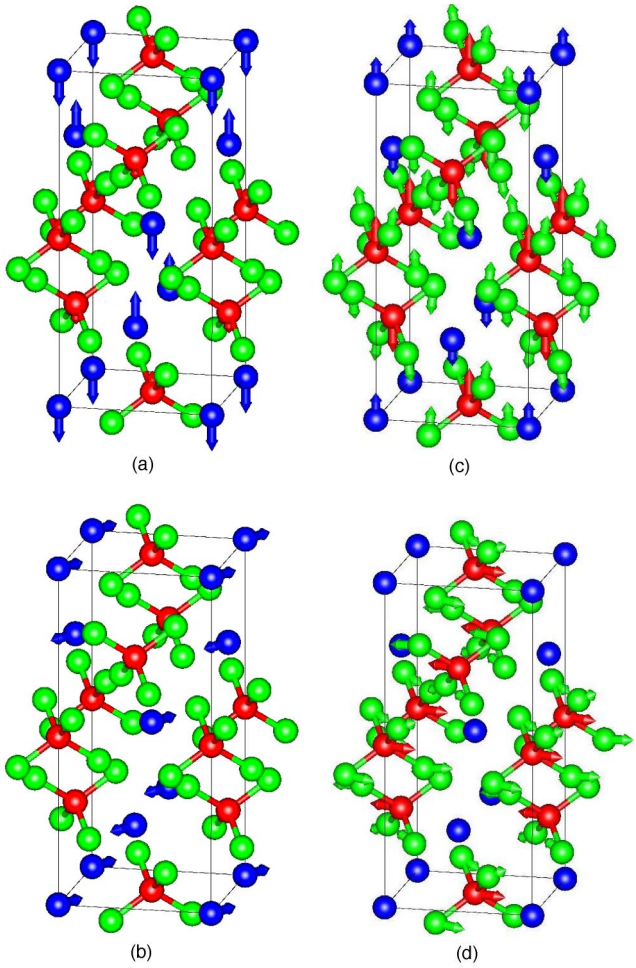

FIG. 7. (Color online) Translational modes in $NaAlH_4$. Red (Al) atoms are tetrahedrally coordinated with green (H) atoms.

equilibrium structural properties, as discussed below.

It is evident from Figs. 7–10 that the separation into four phonon mode groups, translational, librational, Al-H bending and Al-H stretching, is indeed justified. Of particular interest are the former two, since they correspond to low-energy vi-

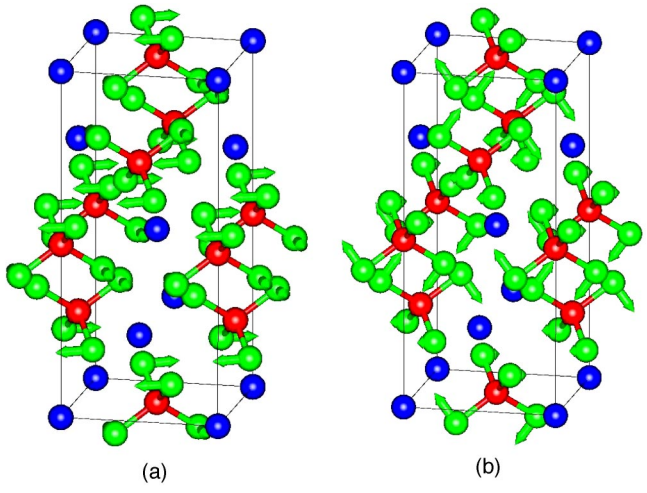

FIG. 8. (Color online) Librational modes in $NaAlH_4$.

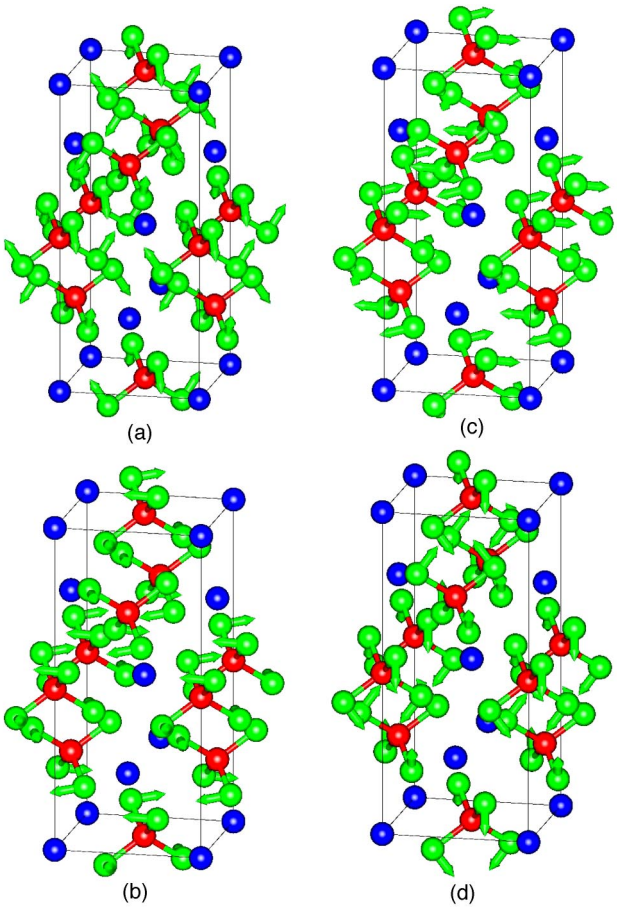

FIG. 9. (Color online) Al-H bending modes in $NaAlH_4$.

brations that were found to exhibit considerable softening upon approaching the melting point. All translational modes in Fig. 7 correspond to simple motions of Na ions and AlH_4 groups relative to each other. The librational modes, shown in Fig. 8, exhibit rigid rotations of the AlH_4^{-1} tetrahedra along the axis that are either parallel to the tetragonal c direction (A_g mode) or lie within the (xy) plane (E_g mode). The dramatic softening of the translational and librational modes near the melting point, and the absence of any noticeable softening in the Al-H bending and stretching modes shown in Figs. 9 and 10, point to a melting mechanism where AlH_4^{-1} remains as a stable structural unit up to and beyond T_m. Since any reaction path for dissociating the AlH_4^{-1} unit must necessarily involve a linear combination of the Al-H bending and stretching modes, it is natural to hypothesize that breaking up (or rebuilding) the AlH_4^{-1} units is the reaction bottleneck for hydrogen release (absorption) in $NaAlH_4$. As argued in the following section, the role of Ti catalyst could be to facilitate the breakup of AlH_4^{-1} units and to reform some of them as AlH_6, as required by the two-step reactions (1) and (2).

The calculated dielectric properties are given in Table II. The Born effective charges indicate that $NaAlH_4$ is a highly ionic compound where the Na atoms are completely stripped of their valence electrons, and Al atoms partially so. This further supports the analysis of the bonding charge distribution and electronic band structure presented in Ref. 2, where

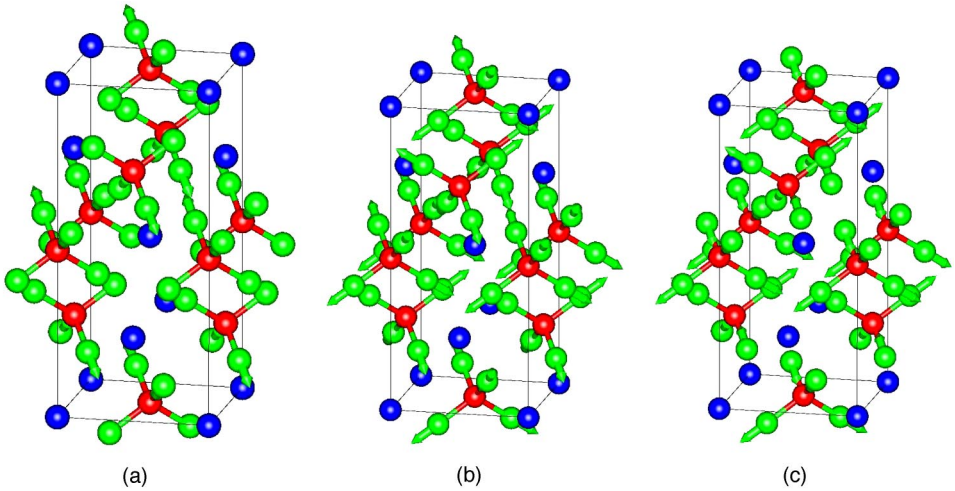

FIG. 10. (Color online) Al-H stretching modes in $NaAlH_4$.

the Al-H bond was characterized as polar covalent. The calculated anisotropy of the dielectric tensor $\epsilon^{\infty}_{\alpha\beta}$ is mild, which is again consistent with the relatively isotropic shape of the band structure of this compound.

The calculated phonon mode Grüneisen parameters, listed in Table I, show that the low-energy translational and librational modes indeed soften most upon lattice expansion, as expected. In contrast, the Al-H bending and stretching mode Grüneisen parameters are much smaller, indicating that the bonding within the AlH_4^{-1} unit is relatively unaffected by lattice expansion. Furthermore, the magnitude of the calculated Grüneisen parameters suggests that the observed frequencies would decrease by approximately 1% for each 1% change in the lattice parameter. Using our calculated estimate of the lattice thermal expansion, shown in Fig. 11, this would account for only an $\approx$0.5% decrease in phonon frequencies over the temperature interval shown in Fig. 5. Only the softening of the Al-H bending and stretching modes is consistent with this estimate, while the frequencies of the translational and librational modes show much more dramatic decrease. Therefore, we conclude that the large softening observed in the *in situ* experiment should be attributed to intrinsic anharmonic effects caused by large-amplitude vibrations near the melting point.

When studying compounds with many light atoms per formula unit, it is important to understand the effects of vibrations on the structural properties. This is especially intriguing in light of the results of available theoretical calculations,[2] which have found that the discrepancies between the calculated and experimentally measured lattice parameters are unusually large (with GGA, the values of a and c were predicted to be 0.4% and 2.2% smaller, respectively[2]). We have calculated the effects of zero-point vibrations and thermal expansion as described in Sec. II B using the LDA linear response method. The results are shown in Fig. 11. The lattice parameters have been expressed as a/a_0 and c/c_0, where a_0 and c_0 are the equilibrium lattice parameters of a static nonvibrating lattice at $T=0$ K, neglecting zero-point motion. It is evident that vibrations have a huge effect on the calculated lattice parameters, increasing the $T=0$ K values by more than 1%, and changing the room-temperature values of a and c by 1.7% and 2.7%, respec-

TABLE II. Born effective charges and dielectric constants for $NaAlH_4$ calculated using the DFT linear response and LDA. Tensors are given in a Cartesian coordinate system where the z axis is pointed along the tetragonal c direction. The Na ion is at $(0,1/4,1/8)$, the Al ion is at $(1/2,3/4,1/8)$, and the H ion is at (0.763,0.597,0.460) in fractional coordinates.

$Z_{\alpha\beta}$(Na)	$\begin{pmatrix} +1.16 & -0.03 & 0 \\ +0.03 & +1.16 & 0 \\ 0 & 0 & +1.04 \end{pmatrix}$
$Z_{\alpha\beta}$(Al)	$\begin{pmatrix} +1.67 & +0.02 & 0 \\ -0.02 & +1.67 & 0 \\ 0 & 0 & +2.12 \end{pmatrix}$
$Z_{\alpha\beta}$(H)	$\begin{pmatrix} -0.73 & -0.05 & +0.06 \\ -0.05 & -0.68 & +0.14 \\ +0.08 & +0.09 & -0.79 \end{pmatrix}$
ϵ^0_{xx}	10.1
ϵ^0_{zz}	9.2
ϵ^{∞}_{xx}	3.5
ϵ^{∞}_{zz}	3.7

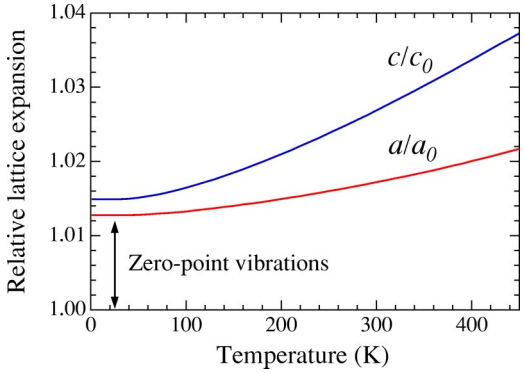

FIG. 11. (Color online) Calculated thermal expansion for $NaAlH_4$, expressed as a/a_0, where a_0 is the lattice parameter of a static nonvibrating lattice, neglecting zero-point motion.

tively. If similar effects hold for the GGA, our results suggest that vibrational expansion could remove the bulk of the discrepancy between the calculated GGA and measured room-temperature values of *c* (from 2.2% smaller to 0.7% smaller), although it should be noted that the agreement between the GGA and experimental numbers for the *a* parameter would be worsened (it would change from 0.4% smaller to 0.8% larger). Finally, our predictions of the lattice thermal expansion between 300 and 450 K agree well with the x-ray data obtained on powdered samples by Gross *et al.*,[11] who found 0.2% and 1% increases in the *a* and *c* parameters, respectively. These results have obvious implications for other complex hydrides with high hydrogen weight fractions, as the ionic zero-point vibrations are expected to result in sizable changes in the calculated lattice parameters. In fact, dynamical effects may account for most of the previously observed discrepancy between the theoretically calculated and experimentally measured lattice parameters.[2,3] Since the simple quasiharmonic Grüneisen treatment seems to "over correct" the *a* parameter, it would be of great interest to apply a computational method with a more accurate theoretical treatment of the quantum nature of the proton. Such a study would allow to estimate the inherent accuracy of the approximate exchange-correlation functionals (LDA and GGA) for complex hydrides.

IV. DISCUSSION

The phonon modes of single crystal $NaAlH_4$ have been investigated. A full polarization analysis of the spectra unambiguously identifies nine of the 13 Raman active modes. The remaining four mode assignments are tentative. *In situ* Raman spectra, taken up to the melting point of $NaAlH_4$, indicate significant softening of the translational and vibrational modes. The bending and stretching modes of the AlH_4^- anion are found to soften less than 1.5%, and indicate that the anion is structurally and dynamically stable up to the melting temperature of the undoped single crystal. These results suggest an obvious explanation for the very low rate of hydrogen release at temperatures below T_{melt} from undoped bulk $NaAlH_4$. Since in a typical applications-oriented sample, doped with 4 at. % $TiCl_3$, the observed decomposition temperatures are roughly 80–90 °C, or 0.75 T_{melt}, this suggests that the catalytic effect of Ti should involve an interaction with the AlH_4^- anion, and a weakening of the Al-H bond strength, resulting in a breakup of the structural unit. Indications that substitutional Ti weakens the Al-H bond, have been offered by the calculations of Íñiguez *et al.*[32] However, the exact location of catalytically active Ti atoms remains a controversial topic that requires furter study.[2,6,9,13,16,33]

ACKNOWLEDGMENTS

This work was funded by the U.S. Department of Energy, Office of Energy Efficiency and Renewable Energy, in the Hydrogen, Fuel Cells & Infrastructure Technologies Program under Contract No. DE-AC36-83CH10093, and Sandia National Laboratories through the Laboratory Directed Research and Development program. Data were fitted using FITYK 0.4.2.

[1] B. Siegel, and G. G. Libowitz, in *Metal Hydrides*, edited by W. M. Mueller, J. P. Blackledge, and G. G. Libowitz (Academic Press, New York, 1968), Chap. 12, p. 545.
[2] V. Ozoliņš, E. Majzoub, and T. Udovic, J. Alloys Compd. **375**, 1 (2004).
[3] A. Aguayo and D. J. Singh, Phys. Rev. B **69**, 155103 (2004).
[4] B. Bogdanovic and M. Schwickardi, J. Alloys Compd. **253-254**, 1 (1997).
[5] B. Bogdanovič, R. Brand, A. Marjanovic, M. Schwickardi, and J. Tolle, J. Alloys Compd. **302**, 36 (2000).
[6] E. Majzoub and K. Gross, J. Alloys Compd. **356-357**, 363 (2003).
[7] A. Finholt, G. Barbaras, G. Barbaras, G. Urry, G. Wartik, and H. Schlesinger, J. Inorg. Nucl. Chem. **1**, 317 (1955).
[8] P. Claudy, B. Bonnetot, G. Chahine, and J. M. Letoffe, Thermochim. Acta **38**, 75 (1980).
[9] G. Sandrock, K. Gross, and G. Thomas, J. Alloys Compd. **339**, 299 (2002).
[10] K. Gross, G. Sandrock, and G. Thomas, J. Alloys Compd. **330-332**, 691 (2002).
[11] K. Gross, S. Guthrie, S. Takara, and G. Thomas, J. Alloys Compd. **297**, 270 (2000).
[12] D. Sun, T. Kiyobayashi, H. Takeshita, N. Kuriyama, and C. Jensen, J. Alloys Compd. **337**, L8 (2002).
[13] B. Bogdanovic, M. Felderhoff, M. Germann, M. Hartel, A. Pommerin, F. Schuth, C. Weidenthaler, and B. Zibrowius, J. Alloys Compd. **350**, 246 (2003).
[14] A. Zaluska, L. Zaluski, and J. Strom-Olsen, J. Alloys Compd. **298**, 125 (2000).
[15] E. Majzoub, R. Stumpf, S. Spangler, J. Herberg, and R. S. Maxwell, in *Hydrogen Storage Materials*, edited by M. Nazri *et al.*, MRS Symposia Proceedings No. 801 (Materials Research Society, Warrendale, PA 2003), p. 153.
[16] C. Weidenthaler, A. Pommerin, M. Felderhoff, B. Bogdanovic, and F. Schuth, Phys. Chem. Chem. Phys. **5**, 5149 (2003).
[17] H. Hagemann, S. Gomes G. Renaudin, and K. Yvon, J. Alloys Compd. **363**, 126 (2004).
[18] S. P. S. Porto, and J. F. Scott, Phys. Rev. **157**, 716 (1967).
[19] J.-C. Bureau, J.-P. Bastide, B. Bonnetot, and H. Eddaoudi, MRS Bull. **20**, 93 (1985).
[20] P. Giannozzi, S. de Gironcoli, P. Pavone, and S. Baroni, Phys. Rev. B **43**, 7231 (1991).
[21] N. Troullier and J. L. Martins, Phys. Rev. B **43**, 1993 (1991).
[22] S. G. Louie, S. Froyen, and M. L. Cohen, Phys. Rev. B **26**, 1738 (1982).
[23] G. Kresse and J. Hafner, J. Phys.: Condens. Matter **6**, 8245 (1994).
[24] G. Kresse and J. Hafner, Phys. Rev. B **47**, R558 (1993).
[25] G. Kresse, Ph.D thesis, Technische Universität Wien, 1993.
[26] G. Kresse and J. Furthmüller, Comput. Mater. Sci. **6**, 15 (1996).

[27] G. Kresse and J. Furthmüller, Phys. Rev. B **54**, 11 169 (1996).
[28] M. E. Tuckerman, D. Marx, M. L. Klein, and M. Parinello, J. Phys. Chem. **104**, 5579 (1996).
[29] V. Bel'skii, B. Bulychev, and A. Golubeva, Russ. J. Inorg. Chem. **28**, 1528 (1983).
[30] J. Lauher, D. Dougherty, and P. Herley, Acta Crystallogr., Sect. B: Struct. Crystallogr. Cryst. Chem. **35**, 1454 (1979).
[31] W. Fateley, *Infrared and Raman Selection Rules for Molecular and Lattice Vibrations: The Correlation Method* (Wiley, New York, 1972).
[32] J. Íñiguez, T. Yildirim, T. J. Udovic, M. Sulic, and C. M. Jensen, Phys. Rev. B **70**, 060101(R) (2004).
[33] J. Graetz, J. Reilly, J. Johnson, A. Ignatov, and T. Tyson, Appl. Phys. Lett. **80**, 500 (2004).